



Universiteit
Leiden
The Netherlands

Modulation of the inflammatory response following myocardial infarction

Pluijmert, N.J.

Citation

Pluijmert, N. J. (2021, June 3). *Modulation of the inflammatory response following myocardial infarction*. Retrieved from <https://hdl.handle.net/1887/3182529>

Version: Publisher's Version

License: [Licence agreement concerning inclusion of doctoral thesis in the Institutional Repository of the University of Leiden](#)

Downloaded from: <https://hdl.handle.net/1887/3182529>

Note: To cite this publication please use the final published version (if applicable).

Cover Page



Universiteit Leiden



The handle <https://hdl.handle.net/1887/3182529> holds various files of this Leiden University dissertation.

Author: Pluijmert, N.J.

Title: Modulation of the inflammatory response following myocardial infarction

Issue Date: 2021-06-03

Phosphorylcholine antibodies preserve cardiac function and reduce infarct size by attenuating the post-ischemic inflammatory response

Niek J. Pluijmer¹
Rob C.M. de Jong^{2,3}
Margreet R. de Vries^{2,3}
Knut Pettersson⁴
Douwe E. Atsma¹
J. Wouter Jukema^{1,3}
Paul H.A. Quax^{2,3}

¹ Department of Cardiology, Leiden University Medical Center, Leiden, The Netherlands

² Department of Surgery, Leiden University Medical Center, Leiden, The Netherlands

³ Einthoven Laboratory for Experimental Vascular Medicine, Leiden University Medical Center, Leiden, The Netherlands

⁴ Athera Biotechnologies, Stockholm, Sweden

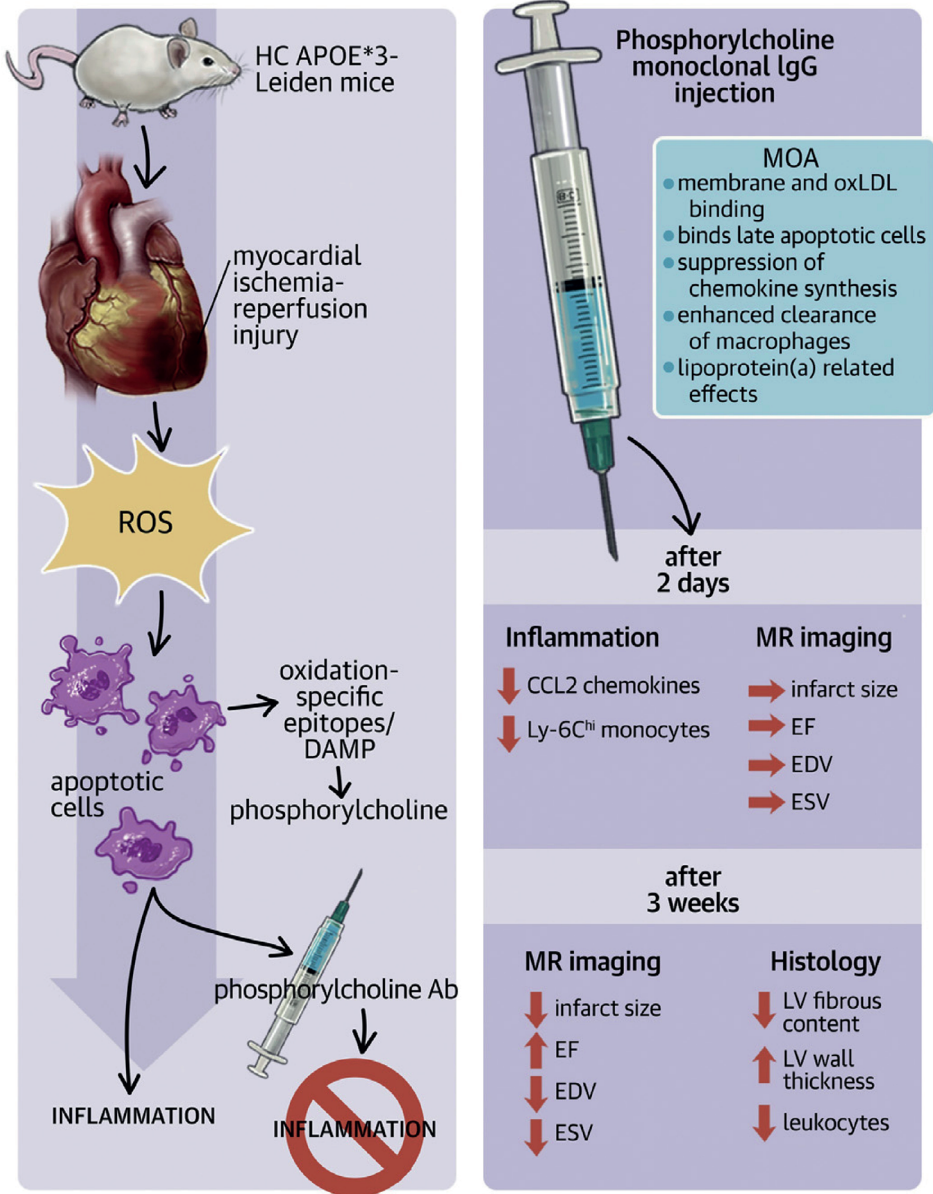
JACC Basic Transl Sci 2020;5(12):1228-39

SUMMARY

Phosphorylcholine monoclonal immunoglobulin G antibody attenuates the immediate post-ischemic inflammatory response by reducing the proinflammatory chemokine (C-C motif) ligand 2 and circulating Ly-6C^{hi} monocytes. This subsequently enhances the post-ischemic repair process resulting in limited adverse cardiac remodeling and preservation of cardiac function. Therefore, phosphorylcholine monoclonal immunoglobulin G antibody therapy may be a valid therapeutic approach against myocardial ischemia-reperfusion injury.

HIGHLIGHTS

- Phosphorylcholine is a proinflammatory epitope exposed on the outer membrane of apoptotic cells.
- This study investigated the modulatory effects of a fully human IgG₁ monoclonal antibody directed against phosphorylcholine (PC-mAb) on myocardial remodeling and cardiac function following myocardial ischemia-reperfusion injury.
- PC-mAb attenuates the immediate post-ischemic inflammatory response by reducing the proinflammatory CCL2 chemokine and circulating Ly-6C^{hi} monocytes. This subsequently enhances the post-ischemic repair process resulting in limited adverse cardiac remodeling and preservation of cardiac function.
- PC-mAb therapy may be a valid therapeutic approach against myocardial ischemia-reperfusion injury.



Visual Abstract: Schematic overview of effects and proposed mechanisms of action of PC-mAb therapy, which attenuates the inflammatory response following MI-R injury resulting in limited adverse LV remodeling and preservation of cardiac function.

INTRODUCTION

Ischemic heart disease remains one of the leading causes of death worldwide¹. Currently, the preferred therapy to treat acute myocardial infarction (MI) is rapid revascularization therapy to salvage myocardium². However, revascularization causes a subsequent problem of myocardial ischemia-reperfusion (MI-R) injury, in which an additional wave of damage is inflicted to the myocardium due to an increased inflammatory response³ and generation of reactive oxygen species⁴, ultimately leading to increased cell death. In a clinical perspective, MI-R injury contributes to adverse cardiac remodeling, which subsequently leads to chronic heart failure, known as an important contributor of morbidity and mortality worldwide³. Currently, ameliorating this post-ischemic inflammatory process and healing of ischemic myocardium to inhibit LV remodeling remains a challenge. Though, large randomized controlled trials as the CANTOS (Canakinumab Antiinflammatory Thrombosis Outcome Study)⁵ and COLCOT (Colchicine Cardiovascular Outcomes)⁶ trials showed the therapeutic potential of anti-inflammatory therapies in reducing cardiovascular events after MI as well as a role for autoantibodies in the prior process of atherogenesis⁷.

The increased inflammatory response during MI-R injury is partially responsible for the increased generation of reactive oxygen species⁴. These reactive oxygen species are responsible for the formation of oxidation-damaged molecules, which can be recognized by the innate immune system. Oxidation-damaged molecules are recognized by the innate immune system via oxidation specific epitopes⁸, which can act as endogenous danger-associated molecular patterns and trigger Toll-like receptors, which play an important role in post-MI remodeling^{9,10} or trigger a chronic inflammatory process as atherosclerosis when the innate immune system is dysfunctional or overwhelmed¹¹. In this way, inflammation and reactive oxygen species generation increase each other's adverse effects following MI-R injury and in chronic inflammation.

Following MI-R injury, ischemic cells express oxidation specific epitopes on their outer membrane in the form of oxidized membrane phospholipids. Phosphorylcholine (PC) is the polar head group of the membrane phospholipid phosphatidylcholine and an example of such an oxidation specific epitope, which is an epitope on apoptotic cells but, interestingly, not on viable cells. Furthermore, apoptotic cells expressing PC, or other oxidation specific epitopes, when present in high quantities are known for their immunogenic and proinflammatory properties¹². Interestingly, PC is also expressed by oxidized low-density lipoprotein, an important lipoprotein in the development of atherosclerosis due to its pro-inflammatory properties⁸. Plasma levels of oxidized phospholipids present on lipoprotein(a) are in turn related to an increased risk of coronary artery disease events¹³. These PC containing proteins are targeted by innate immunity through recognition by scavenger receptors and natural antibodies¹⁴.

Natural antibodies against PC, in mice known as EO6 or T15 antibodies¹⁵, are capable to inhibit oxidized low-density lipoprotein and apoptotic cell uptake by macrophages *in vitro*¹⁶ and *in vivo*¹⁷. However, with intact effector functions and cascade systems, EO6 enhances efferocytosis

of apoptotic cells *in vivo*^{18,19}. Furthermore, it has been shown that EO6 and T15 antibodies block the proinflammatory effects of PC-expressing oxidation-damaged molecules^{12,20}. In addition, it has been shown that B-1a and B-1b cells produce atheroprotective oxidation specific epitope specific antibodies²¹⁻²³, and sterile inflammation in the spleen initiates oxidation specific epitope specific antibody production by splenic B cells, which reduce the development of atherosclerosis²⁴. Moreover, low concentrations of immunoglobulin M (IgM) PC antibodies are associated with increased risk for cardiovascular diseases²⁵⁻²⁷, and acute coronary syndrome patients with low PC antibody levels experience a worsened prognosis²⁸. Active and passive immunization with antibodies against PC reduces atherosclerosis development^{29,30} and vein graft plaque size³¹. Recently, transgenic mice with high levels of a single chain variable fragment of EO6 were shown to reduce infarct size (IS) following MI-R³². Altogether, these data indicate that blocking PC using IgM antibodies may be an interesting approach to treat cardiovascular disease. However, IgM antibodies are not optimal for therapeutic use, because they are, compared to IgG antibodies, rapidly eliminated from plasma, unstable, relatively expensive, and difficult to produce.

Previously we developed PC monoclonal IgG antibody (PC-mAb), a fully human IgG₁ against human PC with anti-inflammatory properties, which reduces accelerated atherosclerosis development³³. Moreover, recently we were able to demonstrate that this antibody preserves coronary vascular function and attenuates vascular ¹⁸F-fluorodeoxyglucose uptake in atherosclerotic mice³⁴. In the current study, we used PC-mAb to investigate its long-term effect against MI-R injury with special attention to the development of heart failure. This study was performed in a model trying to resemble the clinical setting of patients experiencing from MI-R injury as a result of urgent revascularization therapy after a temporary thrombotic occlusion of a coronary artery due to an atherosclerotic plaque rupture. Therefore, we used a MI-R model in hypercholesterolemic APOE*3-Leiden mice starting treatment just after reperfusion with a follow-up period of 3 weeks.

METHODS

MI-R injury was induced in 12- to 14-week-old female APOE*3-Leiden mice as described previously³⁵. Subsequently mice were treated with 10 mg/kg PC-mAb (also known as ATH3G10) (Athera Biotechnologies AB, Stockholm, Sweden) every third day or NaCl 0.9% w/v as a control (vehicle) intraperitoneally. Sham operated animals were operated similarly but without ligation of the left anterior descending coronary artery, and received injections with NaCl 0.9% w/v. After 2 days and 3 weeks, LV function and IS were assessed by cardiac magnetic resonance (CMR) imaging. Three weeks post-reperfusion, LV fibrous content and LV wall thickness were evaluated histologically. Local inflammatory response was investigated 2 days and 3 weeks after MI-R injury using immunohistochemistry. The systemic inflammatory response was analyzed using enzyme-linked immunosorbent assay and fluorescence-activated cell sorting. All animal

experiments were approved by the Institutional Committee for Animal Welfare of the Leiden University Medical Center (LUMC). For further details see the Supplemental Appendix.

Statistical analysis

Values were expressed as mean \pm SEM. Comparisons of parameters between the sham, PC-mAb, and vehicle groups were made using 1- or 2-way analysis of variance (ANOVA) with repeated measures and Tukey's post hoc correction for multiple pairwise comparisons. Comparisons between PC-mAb and vehicle were made using unpaired Student's t-tests. A value of $p < 0.05$ was considered to represent a significant difference. All statistical procedures were performed using IBM SPSS 26.0 (IBM Corporation, Armonk, New York) and GraphPad Prism 8.0 (Graph-Pad Software, San Diego, California).

RESULTS

Animal characteristics, PC-mAb concentrations, and cellular mechanisms

Body weight, heart weight, total plasma cholesterol, and triglyceride concentrations were not affected following PC-mAb treatment (Table 1). To confirm that the observed effects are the result of PC-mAb treatment, we measured circulating PC-mAb levels 2 days and 3 weeks after MI-R injury. PC-mAb was not detectable in the sham and vehicle group at both time points. In the PC-mAb treated group, PC-mAb levels were 45 ± 10 $\mu\text{g/ml}$ after 2 days and 40 ± 10 $\mu\text{g/ml}$ after 3 weeks, endorsing the absence of an immune response against PC-mAb. During the development and production process, PC-mAb was shown to bind late apoptotic cells with strong affinity

	T (wk)	sham	MI-R vehicle	MI-R PC-mAb	p-value overall X ² test
<i>N</i>		13	15	14	
TC (mmol/L)	0	17.5 \pm 1.7	16.8 \pm 1.3	17.4 \pm 1.0	0.932
	3	13.1 \pm 1.1	14.0 \pm 1.2	12.2 \pm 0.5	0.388
TG (mmol/L)	0	2.5 \pm 0.2	2.6 \pm 0.2	3.0 \pm 0.2	0.109
	3	2.4 \pm 0.2	1.8 \pm 0.1 [‡]	1.6 \pm 0.1 [§]	0.005
BW (g)	0	20.7 \pm 0.5	21.1 \pm 0.4	21.5 \pm 0.3	0.361
	3	19.6 \pm 0.3	20.2 \pm 0.4	20.8 \pm 0.3	0.076
HW (mg)	3	144 \pm 8	140 \pm 7	123 \pm 2	0.053
HW/BW ratio (mg/g)	3	7.3 \pm 0.3	6.9 \pm 0.3	5.9 \pm 0.1 ^{*,†}	0.002

Table 1: Plasma lipid profiles and animal characteristics. BW = body weight; HW = heart weight; MI-R = myocardial ischemia-reperfusion; PC-mAb = phosphorylcholine monoclonal immunoglobulin G antibody; TC = total plasma cholesterol; TG = triglycerides. Values are mean \pm SEM. * $p = 0.025$ vs. vehicle, † $p = 0.002$ vs. sham, ‡ $p = 0.037$ vs. sham, § $p = 0.004$ vs. sham.

(Supplemental Figure 1). In addition, cultured peripheral blood mononuclear cells isolated from human blood treated with oxidized low-density lipoprotein showed suppression of chemokine (C-C motif) ligand 2 (CCL2) production levels following concomitant treatment with PC-mAb (Supplemental Figure 2).

Contrast-enhanced CMR assessed infarct size

First, we assessed baseline IS 2 days post MI-R injury using contrast-enhanced CMR imaging. No difference was observed between PC-mAb ($28.3 \pm 1.4\%$) compared with vehicle ($30.6 \pm 2.1\%$) treatment (Figure 1A). Three weeks after MI-R injury, IS was significantly reduced in the PC-mAb group ($12.8 \pm 1.2\%$) compared with the vehicle group ($18.3 \pm 1.1\%$; $p=0.002$). Likewise, absolute IS in the PC-mAb and vehicle groups was similar 2 days after MI-R (16.2 ± 1.0 mg vs. 16.7 ± 1.3 mg) (Figure 1B) but was significantly reduced 3 weeks after MI-R in the PC-mAb group (6.3 ± 0.6 mg) compared with the vehicle group (8.6 ± 0.5 mg; $p=0.006$). Noninfarcted myocardium (Figure

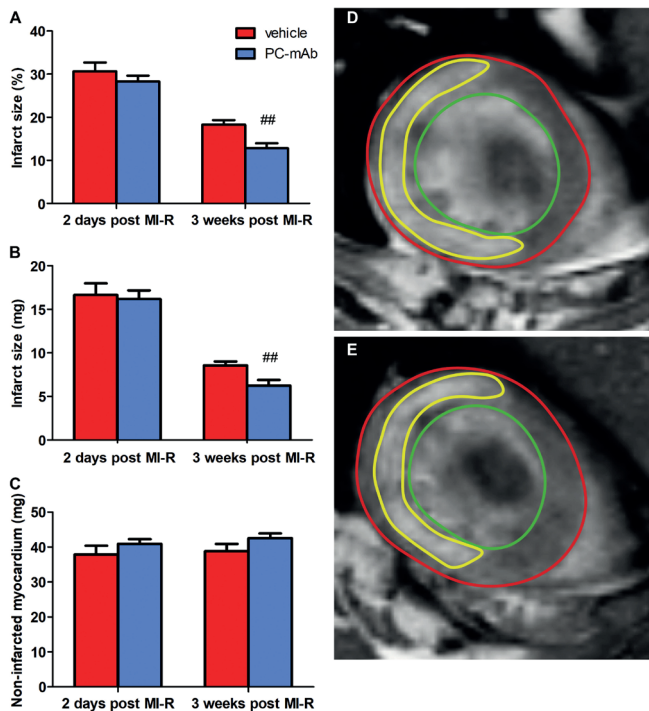


Figure 1: Quantification of infarct size using contrast-enhanced cardiac magnetic resonance imaging. Infarct size was measured at baseline (2 days following MI-R injury) and at sacrifice (3 weeks post MI-R), and infarct size is quantified as percentage of the left ventricular (LV) mass (A) or as absolute mass of the infarcted myocardium (B; $n = 14$ to 15 per group). Representative mass of the noninfarcted myocardium (C). Representative Gd-DPTA-enhanced magnetic resonance images 2 days post MI-R injury of vehicle-treated (D) and PC-mAb therapy-treated (E) mice. Red line indicates epicardial border, green line indicates endocardial border and yellow line indicates infarct area. Values are mean \pm SEM. ## $p < 0.01$ vs. vehicle.

1C) was not significantly different between the PC-mAb and vehicle groups after both 2 days (40.8 ± 1.4 mg vs. 37.9 ± 2.5 mg) and 3 weeks (42.5 ± 1.4 mg vs. 38.8 ± 2.1 mg). As expected, some amount of infarct healing was observed in both groups, as IS was significantly smaller 3 weeks after MI-R when compared with 2 days after MI-R ($p < 0.001$) as a result of transitory early infarct edema. Taken together, PC-mAb treatment seems to significantly decrease IS 3 weeks after MI-R injury.

LV dilatation and function

To investigate the effect of PC-mAb treatment on LV dilatation and function, we made serial cine MR images 2 days and 3 weeks post MI-R injury. Two days after MI-R end-diastolic volume (EDV) (Figure 2A) was not affected following PC-mAb treatment (30.8 ± 0.9 μ l) when compared with sham (28.7 ± 1.2 μ l) and vehicle (34.4 ± 2.3 μ l). However, 3 weeks after MI-R, PC-mAb treatment resulted in significantly smaller EDV compared with vehicle treatment (33.7 ± 1.4 μ l vs. 44.4 ± 2.4 μ l; $p < 0.001$), which was statistically not different from the EDV of sham animals (30.4 ± 1.2 μ l). End-systolic volume (ESV) (Figure 2B) was significantly increased 2 days after MI-R in both the vehicle (19.4 ± 2.0 μ l; $p < 0.001$) and PC-mAb (14.7 ± 0.7 μ l; $p = 0.047$) groups compared with the sham group (9.4 ± 0.8 μ l), while no significant difference could be observed between the vehicle and PC-mAb groups ($p = 0.066$). Interestingly, 3 weeks post MI-R, ESV was markedly reduced following PC-mAb treatment (15.5 ± 0.9 μ l) compared with vehicle treatment

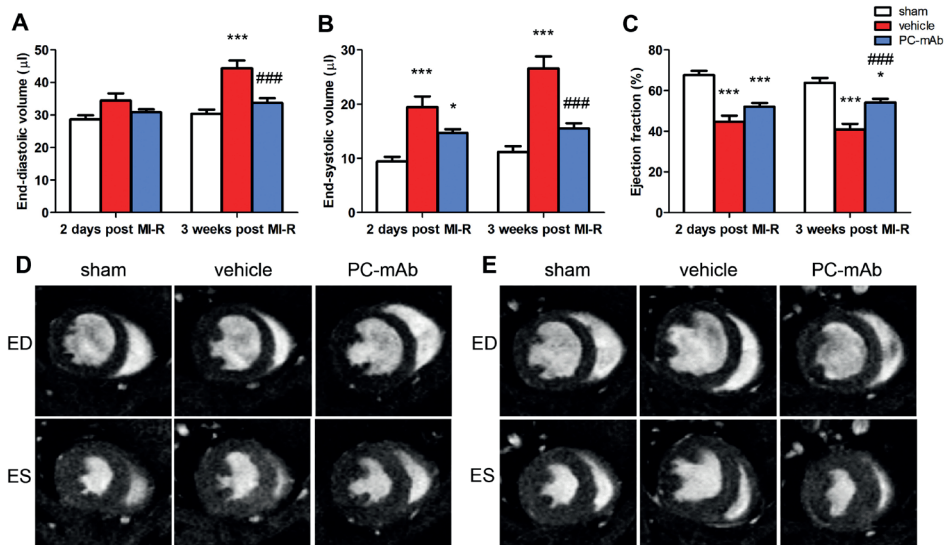


Figure 2: Quantification of LV volumes and function using cardiac magnetic resonance imaging. Left ventricular (LV) volumes, end-diastolic volume (A) and end-systolic volume (B), and function, ejection fraction (C), were assessed 2 days and 3 weeks after MI-R ($n = 12$ to 15 per group). Representative transversal short-axis magnetic resonance images at end-diastole (ED) and end-systole (ES) 2 days (D) and 3 weeks (E) after MI-R in the sham, vehicle, and PC-mAb groups. Values are mean \pm SEM. ### $p < 0.001$ vs. vehicle, * $p < 0.05$, *** $p < 0.001$ both vs. sham.

($26.6 \pm 2.2 \mu\text{l}$; $p < 0.001$), while no significant difference was observed when compared with sham treatment ($11.2 \pm 1.0 \mu\text{l}$; $p = 0.123$). Taken together, these results suggest that PC-mAb treatment prevents LV dilatation to a level comparable to animals without MI-R injury.

Ejection fraction (EF) as a measure of LV function (Figure 2C) was significantly decreased 2 days post MI-R injury in both the vehicle ($44.7 \pm 3.0\%$; $p < 0.001$) and PC-mAb ($52.1 \pm 1.8\%$; $p < 0.001$) groups when compared with the sham group ($67.6 \pm 2.1\%$), while no significant difference was observed between vehicle and PC-mAb treatment ($p = 0.072$). Three weeks after MI-R, EF was still decreased in both the vehicle ($40.8 \pm 2.9\%$; $p < 0.001$) and PC-mAb ($54.1 \pm 1.8\%$, $p = 0.020$) groups when compared with the sham group ($63.9 \pm 2.3\%$). However, PC-mAb treatment significantly increased EF compared with vehicle treatment ($p < 0.001$), indicating preservation of LV function by PC-mAb treatment, whereas EF further deteriorated in the vehicle group compared with the day 2 time point.

LV fibrous content and LV wall thickness

To confirm the effect of PC-mAb on contrast-enhanced CMR assessed IS, we measured LV fibrous content, as a measure of IS, using Sirius Red staining. LV fibrous content was significantly reduced following PC-mAb treatment ($12.9 \pm 1.0\%$) compared with vehicle treatment ($19.8 \pm 1.8\%$; $p = 0.004$) (Figure 3A), confirming the earlier obtained CMR data. Accordingly, 3 weeks after MI-R, LV wall thickness (Figure 3B) in the PC-mAb group compared with the vehicle group was increased in the infarct area ($0.87 \pm 0.03 \text{ mm}$ vs. $0.75 \pm 0.04 \text{ mm}$; $p = 0.045$) and border zones ($1.13 \pm 0.02 \text{ mm}$ vs. $1.03 \pm 0.03 \text{ mm}$; $p = 0.041$). LV wall thickness in the interventricular septum was significantly increased in both the PC-mAb ($1.18 \pm 0.04 \text{ mm}$) and vehicle ($1.10 \pm 0.04 \text{ mm}$) groups compared with the sham group ($0.85 \pm 0.04 \text{ mm}$; both $p < 0.001$). These results indicate cardiac hypertrophy, probably caused by compensation of healthy cardiomyocytes to maintain cardiac function.

Local inflammatory response

To unravel the mechanism of PC-mAb treatment against MI-R injury, we investigated leukocyte infiltration 2 days and 3 weeks after MI-R using immunohistochemistry. First, we studied the early leukocyte infiltration 2 days post MI-R in different areas of the LV wall: the interventricular septum, border zones and infarct area (Figure 4A). There were no differences observed in leukocyte infiltration into the interventricular septum between all groups (sham: 4.8 ± 0.7 leukocytes per 0.25 mm^2 , vehicle: 3.3 ± 1.1 leukocytes per 0.25 mm^2 , and PC-mAb: 2.7 ± 0.6 leukocytes per 0.25 mm^2). Compared with the sham group there was an increased number of leukocyte infiltration in the infarct area of the vehicle group (15.8 ± 4.7 leukocytes per 0.25 mm^2 vs. 4.9 ± 0.4 leukocytes per 0.25 mm^2 ; $p = 0.014$) and a trend towards increased leukocyte infiltration in the border zones (7.7 ± 1.6 leukocytes per 0.25 mm^2 vs. 4.8 ± 0.4 leukocytes per 0.25 mm^2). PC-mAb treatment showed a trend towards attenuated leukocyte infiltration in the infarct area and espe-

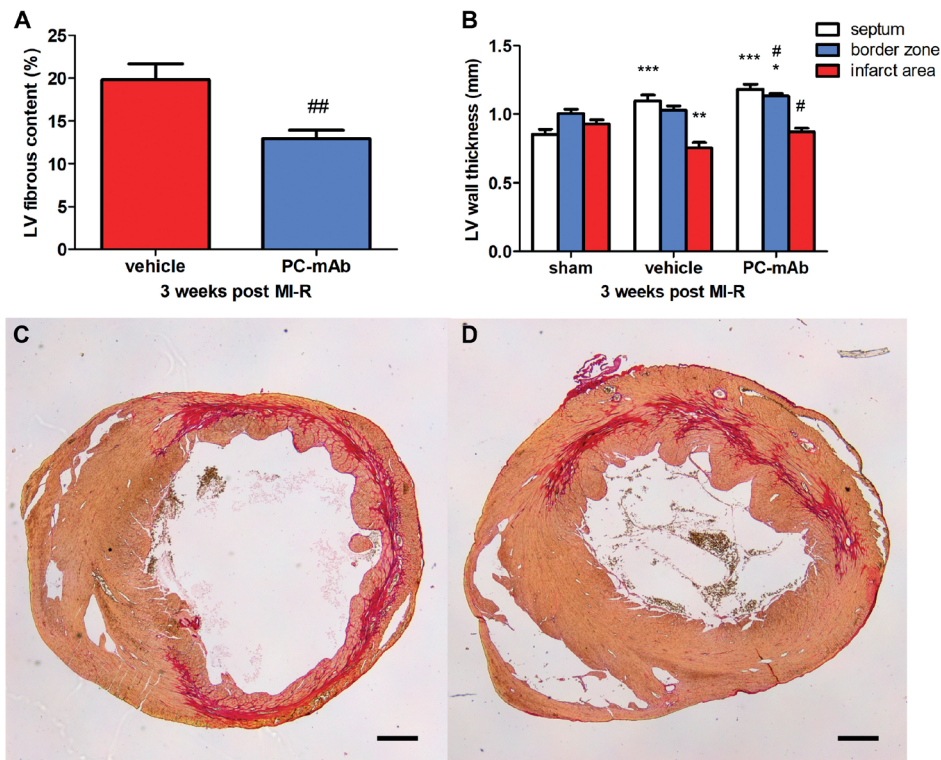


Figure 3: Histological quantification of LV fibrous content and LV wall thickness 3 weeks following MI-R. Left ventricular (LV) fibrous content (A) was measured by Sirius red staining and quantified as the area of the LV occupied by collagen. LV wall thickness (B) was assessed in 3 specific areas: septum, border zone, and infarct area (n = 9 to 10 per group). Representative images of Sirius Red staining of vehicle (C) and PC-mAb treated (D) mice. Scale bar = 500 μ m. Values are mean \pm SEM. [#]p<0.05, ^{##}p<0.01 both vs. vehicle, *p<0.05, **p<0.01, ***p<0.001 all vs. sham.

cially in the border zones (9.5 ± 1.6 leukocytes per 0.25 mm^2 and 4.2 ± 0.6 leukocytes per 0.25 mm^2 ; $p=0.153$ and $p=0.080$, consecutively).

Next, we investigated the leukocyte infiltration 3 weeks post MI-R injury in the same areas as mentioned previously (Figure 4B). In line with previous observations³⁶, leukocyte infiltration was found in the infarcted and noninfarcted myocardium. We observed a significant reduction of leukocyte infiltration in all areas following PC-mAb treatment compared with vehicle (septum: 0.8 ± 0.1 vs. 3.2 ± 0.7 leukocytes per 0.25 mm^2 ; $p=0.001$; border zones: 1.1 ± 0.3 vs. 3.1 ± 0.4 leukocytes per 0.25 mm^2 ; $p<0.001$; infarct area: 0.8 ± 0.2 vs. 3.4 ± 0.7 leukocytes per 0.25 mm^2 ; $p<0.001$), while no differences were observed between the PC-mAb and sham group (septum: 1.2 ± 0.3 leukocytes per 0.25 mm^2 ; border zones: 1.0 ± 0.2 leukocytes per 0.25 mm^2 ; infarct area: 0.8 ± 0.1 leukocytes per 0.25 mm^2). Taken together, these results indicate that PC-mAb treatment reduces local leukocyte infiltration.

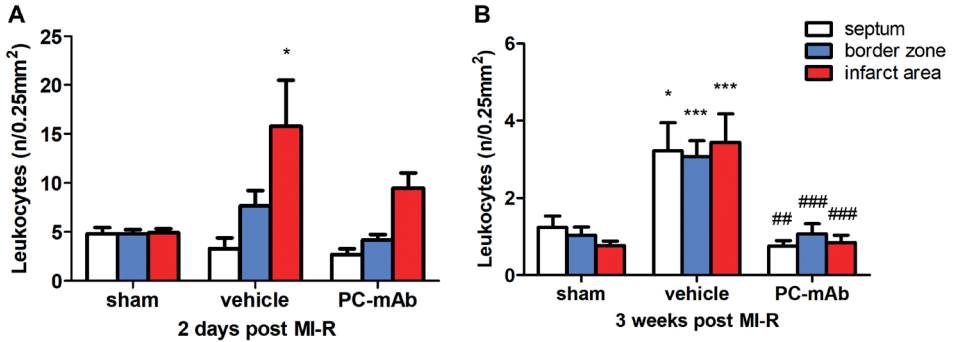


Figure 4: Histological quantification of the local inflammatory response. The number of CD45-positive cells (leukocytes) were counted per specific area (septum, border zone, and infarct area), as a measure of local inflammation. Each bar represents the average number of leukocytes per field of view in the specific areas 2 days post MI-R (A: n = 3 to 5 per group) and 3 weeks post MI-R (B: n = 9 to 10 per group). Values are mean \pm SEM. ##p<0.01, ###p<0.001 both vs. vehicle, *p<0.05, ***p<0.001 both vs. sham.

Systemic inflammatory response

To investigate the effect of PC-mAb treatment on the systemic inflammatory response after MI-R injury, we analyzed serum CCL2 levels 2 days and 3 weeks post MI-R injury. Two days after MI-R, CCL2 levels (Figure 5A) were significantly reduced following PC-mAb treatment (13.4 ± 10.0 pg/ml) compared with both vehicle (74.3 ± 6.6 pg/ml; $p=0.007$) and sham (80.5 ± 14.5 pg/ml; $p=0.002$). Three weeks after MI-R, the effect of PC-mAb treatment on CCL2 levels was less obvious (Figure 5B). Although not significantly, CCL2 levels were decreased following PC-mAb treatment (20.1 ± 7.5 pg/ml) compared with the vehicle (54.3 ± 6.0 pg/ml) and sham (64.9 ± 21.3 pg/ml) groups.

Finally, we investigated the effect of PC-mAb treatment on circulating monocytes 2 days after MI-R. The percentage circulating monocytes (of total leukocytes) was significantly increased following MI-R injury in the vehicle group ($4.3\pm 0.8\%$) compared with the sham group ($2.0\pm 0.5\%$; $p=0.030$) (Figure 5C), but total circulating monocytes were not significantly reduced following PC-mAb treatment ($2.5\pm 0.4\%$; $p=0.090$) as compared with vehicle treatment. However, the percentage circulating proinflammatory Ly-6C^{hi} monocytes was significantly reduced in the PC-mAb group ($1.2\pm 0.2\%$) compared with the vehicle group ($2.5\pm 0.6\%$; $p=0.017$), while no significant difference was observed when compared with the sham group ($0.8\pm 0.2\%$) (Figure 5D). Regarding the percentage circulating reparative Ly-6C^{lo} monocytes, no significant differences were observed between all groups 2 days after MI-R (sham: $0.9\pm 0.2\%$; vehicle: $1.3\pm 0.5\%$; PC-mAb: $1.0\pm 0.3\%$) (Figure 5E). Taken together, these results suggest that PC-mAb treatment especially reduces the early inflammatory response following MI-R injury.

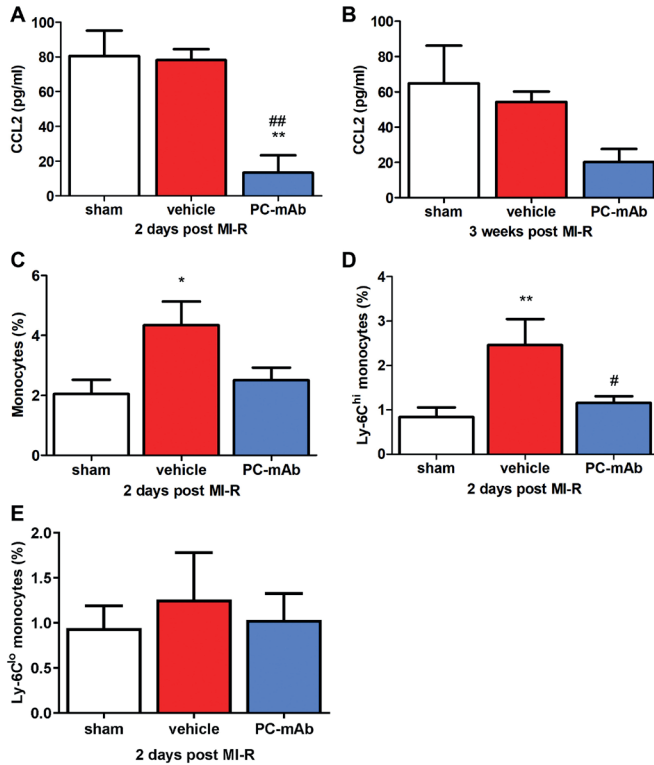


Figure 5: Quantification of the systemic inflammatory response. Serum levels of CCL2 were determined using enzyme-linked immunosorbent assay as a measure of systemic inflammation, 2 days after MI-R (A: n = 4 to 8 per group) and 3 weeks after MI-R (B: n = 9 to 10 per group). Circulating monocytes (C) and different monocyte subsets, Ly-6C^{hi} (D) and Ly-6C^{lo} (E), were determined 2 days after MI-R using fluorescence-activated cell sorting analysis and expressed as percentage of total leukocytes (n = 4 to 8 per group). Values are mean ± SEM. #p < 0.05, ##p < 0.01 both vs. vehicle, *p < 0.05, **p < 0.01, both vs. sham.

DISCUSSION

This study shows a therapeutic effect of PC-mAb treatment after MI-R injury. Administration of PC-mAb after MI-R injury attenuated the early systemic inflammatory response, by reduction of serum CCL2 levels and circulating Ly-6C^{hi} monocytes after 2 days, as well as the late local inflammatory response by decreased myocardial leukocyte infiltration after 3 weeks. This prevented excessive cardiomyocyte cell death, as expressed by a decreased IS and preservation of LV wall thickness, which eventually caused restricted LV dilatation and preserved LV function. Therefore, this fully human monoclonal IgG₁ PC antibody might be a potential future clinical therapeutic agent for the prevention of post-ischemic myocardial remodeling and development of heart failure, and is currently used in a phase 2a randomized double-blind, placebo-controlled multicenter pilot study in patients with acute MI.

Post-ischemic LV remodeling and function

Adverse cardiac remodeling after MI is characterized by an increase of both EDV and ESV, normally followed by a reduced EF³⁷. In this study, we assessed EDV, ESV, and EF and found PC-mAb treatment to significantly restrict the increase in EDV and ESV following MI-R injury accompanied by a significant increase in EF, suggesting limitation of adverse LV remodeling with preservation of LV systolic function.

We investigated the effect of PC-mAb treatment on IS using contrast-enhanced CMR and showed PC-mAb treatment to significantly decrease IS 3 weeks after MI-R injury. Previous research showed that IS is directly related to LV remodeling and clinical outcome following MI^{38,39}. This suggests the observed preservation of LV function to be the result of improved infarct healing as demonstrated by the reduced IS. In addition, we histologically supported this observation demonstrating a decreased LV fibrous content as a measure of IS and increased LV wall thickness following PC-mAb treatment. LV wall thickness is affected following MI because of the loss of viable cardiomyocytes, which are replaced by collagen⁴⁰. The preservation of LV wall thickness might indicate that PC-mAb treatment restricts loss of viable cardiomyocytes. Because IS was not affected 2 days after administration of PC-mAb, the reduced adverse remodeling is likely to be the effect of attenuating the post-ischemic inflammatory response, rather than direct survival of ischemic cardiomyocytes. This is also supported by our data of PC-mAb binding late apoptotic cells as well as suppressed CCL2 levels after treating cultured activated monocytes with PC-mAb. Furthermore, we observed an increase in LV wall thickness in the interventricular septum in both the PC-mAb and vehicle groups, most likely the result of cardiac hypertrophy caused by compensation of healthy cardiomyocytes to maintain cardiac function⁴¹.

Post-ischemic inflammatory response

Inflammation plays an important role in the repair process following MI leading to a matured scar formation⁴². Reperfusion itself causes additional damage to the myocardium by the formation of reactive oxygen species⁴ and accelerates cell membrane damage of cardiomyocytes⁴³, making ischemic-reperfused myocardium amenable to anti-inflammatory interventions. We assessed the effect of PC-mAb treatment on the post-reperfusion inflammatory response by quantification of local infiltration of leukocytes in the LV wall, which was significantly decreased following PC-mAb treatment after 3 weeks. Infarct healing following MI-R injury can be divided into 2 phases, the first being the early inflammatory phase, in which leukocytes are predominantly present in the infarct area playing an important role by removing dead cells and matrix debris, with the second being the reparative phase, in which scar tissue is formed⁴². Besides the infiltration into the infarct area, innate immune cells are also known for their recruitment into the remote myocardium³⁶. Our results suggest PC-mAb treatment to reduce the adverse inflammatory response, while the beneficial early inflammatory response is less affected, as demonstrated by a nonsignificant difference in early leukocyte infiltration after 2 days.

CCL2 is an important chemokine responsible for the recruitment of leukocytes to injured tissue⁴⁴. Even though leukocytes remove possible immunogenic cell components and promote infarct healing after MI, CCL2 knockout mice experience reduced macrophage recruitment to the infarcted myocardium, which resulted in decreased adverse ventricular remodeling following MI-R injury⁴⁵. In agreement with the previously mentioned study, we demonstrated that PC-mAb treatment resulted in significant reduction of CCL2 serum levels 2 days after MI-R injury. Previously, we demonstrated PC-mAb to reduce CCL2 production of monocytes stimulated with oxidized low-density lipoprotein in vitro and CCL2 expression in cuffed femoral arteries in vivo³³. Systemic CCL2 levels are increased in APOE*3-Leiden mice when fed a high-fat diet⁴⁶. We assume that PC-mAb is capable of binding to PC-expressing cells, thereby attenuating the initial immediate systemic inflammatory response or proinflammatory reaction, as observed by reduced CCL2 levels, and subsequently enhances the repair process mediated by M2 macrophages, also supported by the reduced CCL2 levels following PC-mAb treatment of cultured activated monocytes. This finally contributed to the reduction of adverse LV remodeling and preservation of systolic function.

In addition, we observed a decrease of the percentage of monocytes in blood following PC-mAb treatment 2 days after reperfusion. As mentioned previously, infarct healing can be divided in 2 different phases in which both phases a different subset of monocytes plays its own specific role. In the inflammatory phase, proinflammatory Ly-6C^{hi} monocytes, which can differentiate into proinflammatory M1 macrophages, contribute by clearing the infarct site from necrotic cells and matrix debris. In the reparative phase, anti-inflammatory Ly-6C^{lo} monocytes, which can differentiate into repair associated M2 macrophages, play an important role in scar formation and infarct healing⁴². In this study we observed a decrease in Ly-6C^{hi} monocytes, but not in Ly-6C^{lo} monocytes. Thus, despite Ly-6C^{hi} monocytes play an important role in clearing the infarct site from cell debris, we found a beneficial effect on infarct healing and LV function following a PC-mAb induced reduction of circulating Ly-6C^{hi} monocytes. In agreement, it has been shown that hypercholesterolemia results in increased numbers of Ly-6C^{hi} monocytes⁴⁷, thereby influencing infarct healing and cardiac function following MI⁴⁸⁻⁵⁰. Furthermore, hypercholesterolemia affects MI-R injury in mice⁵¹⁻⁵³ and it is an important risk factor of MI in human⁵⁴. Vice versa, MI has been shown to accelerate atherosclerosis⁵⁵ indicating important interactions between both inflammatory processes. This makes them both amenable to anti-inflammatory and immunomodulatory treatment⁵⁶.

Upon a myocardial ischemic event, affected cardiomyocytes can undergo apoptosis⁵⁷, thereby expressing oxidation specific epitopes, like PC, on their outer membrane⁵⁸, which are immunogenic¹². Previous research showed that natural and monoclonal EO6/T15 antibodies against PC are capable to bind apoptotic cells and oxidized low-density lipoprotein^{16,58,59} thereby dampening the inflammatory response^{12,17}. Therefore, we postulate that PC-mAb tempers the immediate systemic inflammatory response following MI-R injury by binding PC-expressing cells before they trigger the innate immune system and enhances the repair process mediated

by M2 macrophages, finally preventing cardiomyocyte cell death and increasing apoptotic cell clearance, which subsequently leads to reduced adverse cardiac remodeling and preservation of cardiac function.

Study Limitations

Although using a translational animal model considering a hypercholesterolemic phenotype and MI-R injury following rapid reperfusion to attempt mimicking the clinical setting, additional human studies are needed to test the clinical relevance of PC-mAb therapy. Further research in atherosclerotic large animal models with human-like plaques or human atherosclerotic patients is needed to investigate the effect on atherosclerotic plaque development. In addition, as a result of the multiple effects of PC-mAb such as direct cellular membrane binding, oxidized low-density lipoprotein binding with inhibition of Toll-like receptor 4 mediated activation, lipoprotein(a)-related effects, and effects via apoptosis, the exact cellular mechanisms remain partially uncertain, although positive clinical effects seem likely. Until now, phase 1 studies showed good safety and tolerability and currently a phase 2a, placebo-controlled, double-blind, randomized multicenter pilot study in patients with acute MI is running. In this study we used a fully human IgG monoclonal antibody in a murine MI-R model, however, previous research confirmed the absence of an immune response. So thus far, PC-mAb therapy seemed safe and promising regarding translation towards the clinical situation.

CONCLUSIONS

PC-mAb treatment attenuates the post-ischemic inflammatory response following MI-R injury as demonstrated by a reduction of systemic CCL2 levels and circulating Ly-6C^{hi} monocytes resulting in impaired myocardial leukocyte infiltration and preservation of LV wall thickness. In a hypercholesterolemic mouse model mimicking the clinical setting, this resulted in limited adverse cardiac remodeling, with a decreased infarct size causing reduced LV dilatation, preventing development of heart failure and preserving LV function. Therefore, PC-mAb therapy may be a valid therapeutic approach against MI-R injury.

Perspectives

Competency in medical knowledge: The therapeutic potential of anti-inflammatory therapies is of interest in reducing cardiovascular events following MI. Antibodies against phosphorylcholine are known to have anti-inflammatory properties by blocking the uptake of oxidized low-density lipoprotein by macrophages.

Translational outlook: PC-mAb therapy may be a valid therapeutic approach against MI-R injury.

REFERENCES

1. McAloon CJ, Boylan LM, Hamborg T, et al. The changing face of cardiovascular disease 2000-2012: An analysis of the world health organisation global health estimates data. *Int J Cardiol* 2016;224:256-64.
2. Bagai A, Dangas GD, Stone GW, Granger CB. Reperfusion strategies in acute coronary syndromes. *Circ Res* 2014;114:1918-28.
3. Ibanez B, Heusch G, Ovize M, Van de Werf F. Evolving therapies for myocardial ischemia/reperfusion injury. *J Am Coll Cardiol* 2015;65:1454-71.
4. Bagheri F, Khori V, Alizadeh AM, Khalighfard S, Khodayari S, Khodayari H. Reactive oxygen species-mediated cardiac-reperfusion injury: Mechanisms and therapies. *Life Sci* 2016;165:43-55.
5. Ridker PM, Everett BM, Thuren T, et al. Antiinflammatory Therapy with Canakinumab for Atherosclerotic Disease. *N Engl J Med* 2017;377:1119-31.
6. Tardif JC, Kouz S, Waters DD, et al. Efficacy and Safety of Low-Dose Colchicine after Myocardial Infarction. *N Engl J Med* 2019;381:2497-2505.
7. Iseme RA, McEvoy M, Kelly B, et al. A role for autoantibodies in atherogenesis. *Cardiovasc Res* 2017;113:1102-12.
8. Miller YI, Choi SH, Wiesner P, et al. Oxidation-specific epitopes are danger-associated molecular patterns recognized by pattern recognition receptors of innate immunity. *Circ Res* 2011;108:235-48.
9. Arslan F, Smeets MB, Riem Vis PW, et al. Lack of fibronectin-EDA promotes survival and prevents adverse remodeling and heart function deterioration after myocardial infarction. *Circ Res* 2011;108:582-92.
10. Timmers L, Sluijter JP, van Keulen JK, et al. Toll-like receptor 4 mediates maladaptive left ventricular remodeling and impairs cardiac function after myocardial infarction. *Circ Res* 2008;102:257-64.
11. Binder CJ, Papac-Milicevic N, Witztum JL. Innate sensing of oxidation-specific epitopes in health and disease. *Nat Rev Immunol* 2016;16:485-97.
12. Chang MK, Binder CJ, Miller YI, et al. Apoptotic cells with oxidation-specific epitopes are immunogenic and proinflammatory. *J Exp Med* 2004;200:1359-70.
13. Tsimikas S, Mallat Z, Talmud PJ, et al. Oxidation-specific biomarkers, lipoprotein(a), and risk of fatal and nonfatal coronary events. *J Am Coll Cardiol* 2010;56:946-55.
14. Shaw PX, Horkko S, Chang MK, et al. Natural antibodies with the T15 idiotype may act in atherosclerosis, apoptotic clearance, and protective immunity. *J Clin Invest* 2000;105:1731-40.
15. Palinski W, Horkko S, Miller E, et al. Cloning of monoclonal autoantibodies to epitopes of oxidized lipoproteins from apolipoprotein E-deficient mice. Demonstration of epitopes of oxidized low density lipoprotein in human plasma. *J Clin Invest* 1996;98:800-14.
16. Chang MK, Bergmark C, Laurila A, et al. Monoclonal antibodies against oxidized low-density lipoprotein bind to apoptotic cells and inhibit their phagocytosis by elicited macrophages: evidence that oxidation-specific epitopes mediate macrophage recognition. *Proc Natl Acad Sci U S A* 1999;96:6353-8.
17. Que X, Hung MY, Yeang C, et al. Oxidized phospholipids are proinflammatory and proatherogenic in hypercholesterolaemic mice. *Nature* 2018;558:301-6.
18. Elkon KB, Silverman GJ. Naturally occurring autoantibodies to apoptotic cells. *Adv Exp Med Biol* 2012;750:14-26.
19. Rahman M, Sing S, Golabkesh Z, et al. IgM antibodies against malondialdehyde and phosphorylcholine are together strong protection markers for atherosclerosis in systemic lupus erythematosus: Regulation and underlying mechanisms. *Clin Immunol* 2016;166-167:27-37.
20. Huber J, Vales A, Mitulovic G, et al. Oxidized membrane vesicles and blebs from apoptotic cells contain biologically active oxidized phospholipids that induce monocyte-endothelial interactions. *Arterioscler Thromb Vasc Biol* 2002;22:101-7.
21. Kyaw T, Tay C, Krishnamurthi S, et al. B1a B lymphocytes are atheroprotective by secreting natural IgM that increases IgM deposits and reduces necrotic cores in atherosclerotic lesions. *Circ Res* 2011;109:830-40.
22. Rosenfeld SM, Perry HM, Gonen A, et al. B-1b Cells Secrete Atheroprotective IgM and Attenuate Atherosclerosis. *Circ Res* 2015;117:e28-e39.
23. Tsiantoulas D, Gruber S, Binder CJ. B-1 cell immunoglobulin directed against oxidation-specific epitopes. *Front Immunol* 2012;3:415.

24. Grasset EK, Duhlin A, Agardh HE, et al. Sterile inflammation in the spleen during atherosclerosis provides oxidation-specific epitopes that induce a protective B-cell response. *Proc Natl Acad Sci U S A* 2015;112:E2030-E2038.
25. de Faire U, Su J, Hua X, et al. Low levels of IgM antibodies to phosphorylcholine predict cardiovascular disease in 60-year old men: effects on uptake of oxidized LDL in macrophages as a potential mechanism. *J Autoimmun* 2010;34:73-9.
26. Gigante B, Leander K, Vikstrom M, et al. Low levels of IgM antibodies against phosphorylcholine are associated with fast carotid intima media thickness progression and cardiovascular risk in men. *Atherosclerosis* 2014;236:394-9.
27. Gronlund H, Hallmans G, Jansson JH, et al. Low levels of IgM antibodies against phosphorylcholine predict development of acute myocardial infarction in a population-based cohort from northern Sweden. *Eur J Cardiovasc Prev Rehabil* 2009;16:382-6.
28. Caidahl K, Hartford M, Karlsson T, et al. IgM-phosphorylcholine autoantibodies and outcome in acute coronary syndromes. *Int J Cardiol* 2013;167:464-9.
29. Binder CJ, Horkko S, Dewan A, et al. Pneumococcal vaccination decreases atherosclerotic lesion formation: molecular mimicry between *Streptococcus pneumoniae* and oxidized LDL. *Nat Med* 2003;9:736-43.
30. Caligiuri G, Khallou-Laschet J, Vandaele M, et al. Phosphorylcholine-targeting immunization reduces atherosclerosis. *J Am Coll Cardiol* 2007;50:540-6.
31. Faria-Neto JR, Chyu KY, Li X, et al. Passive immunization with monoclonal IgM antibodies against phosphorylcholine reduces accelerated vein graft atherosclerosis in apolipoprotein E-null mice. *Atherosclerosis* 2006;189:83-90.
32. Yeang C, Hasanally D, Que X, et al. Reduction of myocardial ischaemia-reperfusion injury by inactivating oxidized phospholipids. *Cardiovasc Res* 2019;115:179-89.
33. de Vries MR, Ewing MM, de Jong RCM, et al. Identification of IgG1 isotype phosphorylcholine antibodies for the treatment of inflammatory cardiovascular diseases. *J Intern Med* 2020.
34. Stähle M, Silvola JMU, Hellberg S, et al. Therapeutic antibody against phosphorylcholine preserves coronary vascular function and attenuates vascular ¹⁸F-FDG uptake in atherosclerotic mice. *JACC Basic Transl Sci* 2020;25:360-373.
35. Michael LH, Ballantyne CM, Zachariah JP, et al. Myocardial infarction and remodeling in mice: effect of reperfusion. *Am J Physiol* 1999;277:H660-H668.
36. Lee WW, Marinelli B, van der Laan AM, et al. PET/MRI of inflammation in myocardial infarction. *J Am Coll Cardiol* 2012;59:153-63.
37. Galli A, Lombardi F. Postinfarct Left Ventricular Remodelling: A Prevailing Cause of Heart Failure. *Cardiol Res Pract* 2016;2016:2579832.
38. Masci PG, Ganame J, Francone M, et al. Relationship between location and size of myocardial infarction and their reciprocal influences on post-infarction left ventricular remodelling. *Eur Heart J* 2011;32:1640-8.
39. McAlindon E, Bucciarelli-Ducci C, Suleiman MS, Baumbach A. Infarct size reduction in acute myocardial infarction. *Heart* 2015;101:155-60.
40. Sutton MG, Sharpe N. Left ventricular remodeling after myocardial infarction: pathophysiology and therapy. *Circulation* 2000;101:2981-8.
41. Shimizu I, Minamino T. Physiological and pathological cardiac hypertrophy. *J Mol Cell Cardiol* 2016;97:245-62.
42. Prabhu SD, Frangogiannis NG. The Biological Basis for Cardiac Repair After Myocardial Infarction: From Inflammation to Fibrosis. *Circ Res* 2016;119:91-112.
43. Hori M, Nishida K. Oxidative stress and left ventricular remodelling after myocardial infarction. *Cardiovasc Res* 2009;81:457-64.
44. Gillitzer R, Goebeler M. Chemokines in cutaneous wound healing. *J Leukoc Biol* 2001;69:513-21.
45. Dewald O, Zymek P, Winkelmann K, et al. CCL2/Monocyte Chemoattractant Protein-1 regulates inflammatory responses critical to healing myocardial infarcts. *Circ Res* 2005;96:881-9.
46. Murphy N, Grimsditch DC, Vidgeon-Hart M, et al. Dietary antioxidants decrease serum soluble adhesion molecule (sVCAM-1, sICAM-1) but not chemokine (JE/MCP-1, KC) concentrations, and reduce atherosclerosis in C57BL but not apoE⁻³ Leiden mice fed an atherogenic diet. *Dis Markers* 2005;21:181-90.
47. Swirski FK, Libby P, Aikawa E, et al. Ly-6Chi monocytes dominate hypercholesterolemia-associated monocytosis and give rise to macrophages in atheromata. *J Clin Invest* 2007;117:195-205.

48. Nahrendorf M, Swirski FK, Aikawa E, et al. The healing myocardium sequentially mobilizes two monocyte subsets with divergent and complementary functions. *J Exp Med* 2007;204:3037-47.
49. Panizzi P, Swirski FK, Figueiredo JL, et al. Impaired infarct healing in atherosclerotic mice with Ly-6C(hi) monocytosis. *J Am Coll Cardiol* 2010;55:1629-38.
50. Pluijmer NJ, den Haan MC, van Zuylen VL, et al. Hypercholesterolemia affects cardiac function, infarct size and inflammation in APOE*3-Leiden mice following myocardial ischemia-reperfusion injury. *PLoS One* 2019;14:e0217582.
51. Girod WG, Jones SP, Sieber N, Aw TY, Lefer DJ. Effects of hypercholesterolemia on myocardial ischemia-reperfusion injury in LDL receptor-deficient mice. *Arterioscler Thromb Vasc Biol* 1999;19:2776-81.
52. Jones SP, Girod WG, Marotti KR, Aw TY, Lefer DJ. Acute exposure to a high cholesterol diet attenuates myocardial ischemia-reperfusion injury in cholesteryl ester transfer protein mice. *Coron Artery Dis* 2001;12:37-44.
53. Scalia R, Gooszen ME, Jones SP, et al. Simvastatin exerts both anti-inflammatory and cardioprotective effects in apolipoprotein E-deficient mice. *Circulation* 2001;103:2598-603.
54. Yusuf S, Hawken S, Ounpuu S, et al. Effect of potentially modifiable risk factors associated with myocardial infarction in 52 countries (the INTERHEART study): case-control study. *Lancet* 2004;364:937-52.
55. Dutta P, Courties G, Wei Y, et al. Myocardial infarction accelerates atherosclerosis. *Nature* 2012;487:325-9.
56. Frostegard J. Immunity, atherosclerosis and cardiovascular disease. *BMC Med* 2013;11:117.
57. Frangogiannis NG. The immune system and cardiac repair. *Pharmacol Res* 2008;58:88-111.
58. Chou MY, Fogelstrand L, Hartvigsen K, et al. Oxidation-specific epitopes are dominant targets of innate natural antibodies in mice and humans. *J Clin Invest* 2009;119:1335-49.
59. Horkko S, Bird DA, Miller E, et al. Monoclonal autoantibodies specific for oxidized phospholipids or oxidized phospholipid-protein adducts inhibit macrophage uptake of oxidized low-density lipoproteins. *J Clin Invest* 1999;103:117-28.

SUPPLEMENTAL MATERIAL

Methods

Animals and diets

All animal experiments were approved by the Institutional Committee for Animal Welfare of the Leiden University Medical Center (LUMC) and conformed to the Guide for the Care and Use of Laboratory Animals (NIH publication No. 85-23, revised 2011). Transgenic female APOE*3-Leiden mice¹, backcrossed for more than 40 generations on a C57Bl/6J background (bred in the animal facility of the LUMC), aged 8-10 weeks at the start of a dietary run-in period were used for this experiment. Mice were fed a semisynthetic Western-type diet supplemented with 0.4% cholesterol (AB Diets, Woerden, The Netherlands) four weeks prior to surgery, which was continued throughout the complete experiment. Mice were housed under standard conditions in conventional cages and received food and water ad libitum.

Plasma lipid analysis

Plasma levels of total cholesterol and triglycerides were determined for randomization one week before surgery. After a 4-hour fasting period, plasma was obtained via tail vein bleeding and assayed for total cholesterol and triglycerides levels using commercially available enzymatic kits according to the manufacturer's protocols (11489232; Roche Diagnostics, Mannheim, Germany, and 11488872; Roche Diagnostics, Mannheim, Germany, respectively).

Surgical myocardial infarction model and PC-mAb injections

MI-R injury was induced at day 0 in 12-14 weeks old female APOE*3-Leiden mice as described previously². Briefly, mice were pre-anesthetized with 5% isoflurane in a gas mixture of oxygen and room air and placed in a supine position on a heating pad. After endotracheal intubation and ventilation (rate 160 breaths/min, stroke volume 190 μ l; Harvard Apparatus, Holliston, MA, USA), mice were kept anesthetized with 1.5-2% isoflurane. Subsequently, a left thoracotomy was performed in the 4th intercostal space and the left anterior descending (LAD) coronary artery was ligated during 45 minutes using a 7-0 Prolene suture knotted on a 2 mm section of a plastic tube. Ischemia was confirmed by myocardial blanching. After 45 minutes of ischemia, permanent reperfusion was established. Subsequently, the thorax was closed in layers with 5-0 Prolene suture and mice were allowed to recover. Analgesia was obtained with buprenorphine s.c. (0.1 mg/kg) pre-operative and 10-12 hours post-operative. After surgery, animals were randomly grouped to receive intraperitoneal injections with 10 mg/kg PC-mAb (ATH3G10, Athera Biotechnologies AB, Stockholm, Sweden) every 3rd day or NaCl 0.9% w/v as a control (vehicle). Sham operated animals were operated similarly but without ligation of the LAD and received intraperitoneal injections with NaCl 0.9% w/v. Injections were administered direct after surgery (approximately 15 minutes after reperfusion) and between 12:00 p.m. and 2:00 p.m. every 3rd day thereafter.

After two days or three weeks, mice were euthanized by bleeding and explantation of the heart under general anesthesia with 1.5-2% isoflurane and heart weight was determined using a digital scale. Next, hearts were immersion-fixed in 4% paraformaldehyde for 24 hours and embedded in paraffin. Blood samples were collected and used for serum analysis. The heart and body weights were measured from all animals.

Cardiac magnetic resonance imaging

LV dimensions and function were assessed two and three weeks after surgery by using a 7-Tesla magnetic resonance imaging (MRI) (Bruker Biospin, Ettlingen, Germany) to obtain contrast-enhanced and cine CMR images. Mice were pre-anesthetized with 5% isoflurane and maintained anesthetized at 1-2% isoflurane. Respiratory rate was monitored by a respiration detection cushion, which was placed underneath the thorax and connected to a gating module to monitor respiratory rate (SA Instruments, Inc., Stony Brook, NY). Image reconstruction was performed using Bruker ParaVision 5.1 software.

Infarct size

To distinguish for any possible treatment effect initial baseline IS was determined at day two using contrast-enhanced CMR imaging after injection of a 150 μ l (0.05 mmol/ml) bolus of gadolinium-DPTA (Gd-DPTA, Dotarem, Guerbet, The Netherlands) via the tail vein. A high-resolution 2D FLASH cine sequence was used to acquire a set of 14 contiguous 0.5 mm slices in short-axis orientation covering the entire heart. Imaging parameters were echo time of 1.9 ms, repetition time of 84.16 ms, field of view of 33 mm², and a matrix size of 192x256.

Mice without visible contrast were excluded from the study as being failed MI procedure. Therapeutic effects regarding IS were determined by repetition of contrast-enhanced CMR imaging at day 21.

LV dimensions and function

LV dimensions were measured at day two and after three weeks with a high-resolution 2D fast gradient echo (FLASH) sequence to acquire a set of contiguous 1 mm slices in short-axis orientation covering the entire long-axis of the heart. Imaging parameters were echo time of 1.49 ms, repetition time of 5.16 ms, field of view of 26 mm², and a matrix size of 144x192.

Image analysis

CMR images were converted to DICOM format and analyzed with the MR Analytical Software System (MASS) for mice (Medis, Leiden, The Netherlands). LV endo- and epicardial borders were delineated manually by an investigator blinded to the experimental groups. End-diastolic and end-systolic phases and the contrast enhanced areas were identified automatically, and the percentage of infarcted myocardium, EDV, ESV, and EF were computed.

LV fibrous content and LV wall thickness

Paraffin-embedded hearts were cut into serial transverse sections of 5 μm along the entire long-axis of the LV. To analyze collagen deposition as an indicator of the fibrotic area, every 50th section of each heart was stained with Sirius Red. LV fibrous content was determined by planimetric measurement of all sections and calculated as fibrotic area divided by the total LV wall surface area including the interventricular septum.

LV wall thickness was measured in five different sections centralized in the infarct area. Per section, wall thickness was analyzed at 3 places equally distributed in the infarct area, both border zones, and 2 places of the interventricular septum. Measurements were performed perpendicular to the ventricular wall. Corresponding areas were used for measurements in the noninfarcted sham group. All measurements were performed by an observer blinded to the groups, using the ImageJ 1.51 software program (NIH, USA).

Myocardial inflammatory response

For analysis of the cardiac inflammatory response a subpopulation was selected, and sections of the mid-infarct region of the heart were stained using antibodies against leukocytes (anti-CD45, 550539; BD Pharmingen, San Diego, CA, USA). The number of leukocytes was expressed as a number per 0.25 mm² in the septum (2 areas), border zones (2 areas), and infarcted myocardium (3 areas). Corresponding areas were used for measurements in the non-infarcted sham group.

Fluorescence-activated cell sorting analysis

To examine the effect of PC-mAb therapy on the acute inflammatory response, mice were euthanized and blood samples were collected at day two. To study the systemic effects whole blood was analyzed for monocytosis. White blood cell counts (WBC, $\times 10^6/\text{ml}$) were measured using a semi-automatic hematology analyzer F-820 (Sysmex; Sysmex Corporation, Etten-Leur, The Netherlands). For fluorescence-activated cell sorting analysis, 35 μl of whole blood was incubated for 30 min on ice with directly conjugated antibodies directed against Ly6C-FITC (AbD Serotec, Dusseldorf, Germany), Ly6G-PE (BD Pharmingen, San Diego, CA, USA), CD11b-APC (BD Pharmingen, San Diego, CA, USA), and CD115-PerCP (R&D Systems, Minneapolis, MN, USA). Monocytes were gated based on their expression profile: CD11b-positive, Ly6G-negative, and CD115-positive. Data was analyzed using FlowJo software (Tree Star Inc.)

CCL2 and PC-mAb ELISA

A PC-mAb ELISA kit (Athera Biotechnologies, Solna, Sweden) was used to determine serum PC-mAb concentrations. To study the effects of PC-mAb on systemic inflammation, an ELISA kit (Cat. No. 555260, BD Biosciences, San Diego, CA, USA) for cytokine concentration of CCL2 was used.

Apoptotic cell binding assays

Jurkat T cells (ATCC) were cultured in RPMI1640 media supplemented with 10% FBS, penicillin (100 U/ml) and streptomycin (100 µg/ml). After blocking with 5% BSA, cells were incubated with 20 µg/ml PC-mAb antibodies in PBS. Anti-streptavidin A2 antibodies were used as isotype control. Apoptosis was induced by overnight incubation with 2 µg/ml staurosporine in culture medium. Cells were incubated with FITC-conjugated goat anti-human IgA, IgG, or IgM, (Thermo), APC- annexin V antibody (BD Biosciences) and propidium iodide. Cells were analyzed by flow cytometry (LSRII, BD Biosciences).

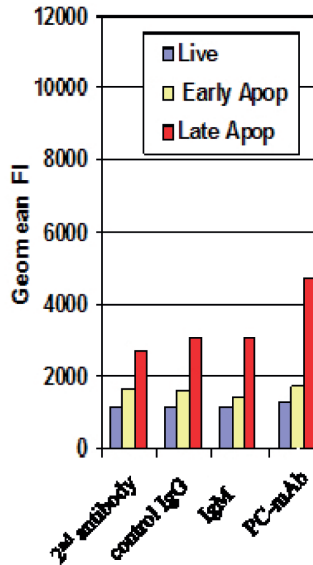
Cell cultures

Peripheral blood mononuclear cells (PBMCs) were isolated from citrated human blood using Ficoll-Paque PLUS (GE Healthcare) according to the instructions of the manufacturer. Monocytes were resuspended in serum free RPMI 1640 medium at density of 8×10^5 cells/ml and 250 µl cell suspension was added into wells of a 96-well plate (2×10^5 cells/well). PBMCs were treated with 2 µg/ml oxLDL (Kalen Biomedical) in the presence or absence of up to 40 nM PC-mAb for 40 hours at 37°C, 5% CO₂.

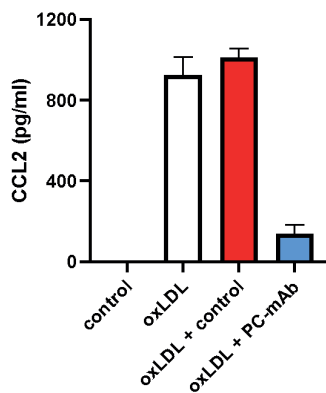
References

1. van den Maagdenberg AM, Hofker MH, Krimpenfort PJ, et al. Transgenic mice carrying the apolipoprotein E3-Leiden gene exhibit hyperlipoproteinemia. *J Biol Chem* 1993;268:10540-10545.
2. Michael LH, Ballantyne CM, Zachariah JP, et al. Myocardial infarction and remodeling in mice: effect of reperfusion. *Am J Physiol* 1999;277:H660-668.

SUPPLEMENTARY FIGURES



Supplemental Figure 1: PC-mAb binding affinity to apoptotic Jurkat T cells. Flow cytometry of antibody affinity for live cells (annexin V-PI-), early apoptotic cells (annexin V+PI-) and late apoptotic cells (annexin V+PI+) expressed as mean fluorescent intensity of each cell population. Affinity of a 2nd antibody, IgG isotype control, murine IgM anti-PC and PC-mAb was tested. PC-mAb was found to bind strongly to late apoptotic Jurkat cells.



Supplemental Figure 2: PC-mAb affecting expression levels of CCL2. Cultured PBMCs isolated from human blood were treated with oxidized low-density lipoprotein (oxLDL) in the presence or absence of PC-mAb with IgG isotype as a control. PC-mAb treatment resulted in a clear suppression of CCL2 levels.

